Carbohydrate Polymers 82 (2010) 663–669

Contents lists available at ScienceDirect

Carbohydrate Polymers

journal homepage: www.elsevier.com/locate/carbpol

NMR relaxometry and rheology of ionic and acid alginate gels

Benito de Celis Alonso[a,1], Phillippa Rayment[b], Elisabetta Ciampi[b], Stephen Ablett[b], Luca Marciani[c], Robin C. Spiller[c], Ian T. Norton[b,2], Penny A. Gowland[a,*]

[a] Sir Peter Mansfield Magnetic Resonance Centre, School of Physics and Astronomy, University of Nottingham, Nottingham NG7 2RD, UK
[b] Unilever Discover, Colworth Science Park, Sharnbrook, Bedford MK44 1LQ, UK
[c] Nottingham Digestive Diseases Centre NIHR Biomedical Research Unit, QMC, Nottingham University Hospitals NHS Trust, University of Nottingham, Nottingham NG7 2UH, UK

ARTICLE INFO

Article history:
Received 9 February 2010
Received in revised form 10 May 2010
Accepted 18 May 2010
Available online 25 May 2010

Keywords:
Alginate
Gel
Microstructure
Nuclear magnetic resonance (NMR)
Rheology
R2

ABSTRACT

The relationship between NMR relaxometry and rheology of acid alginate gels has been investigated *in vitro* and compared to that of ionic alginate gels. The onset and early stages of the gelation process were characterized by the time dependent changes in the storage modulus G' and transverse relaxation rate $R2$ of the water, demonstrating how this NMR parameter can be used as a non-invasive/non-destructive indicator of the formation of these gels. Compression tests on the final gels showed that the acid gels were much weaker. No direct correlation was observed between the final strength of these types of gels and the measured NMR $R2$ values. The results suggest that in MRI studies *in vivo* the $R2$ relaxation rate could provide valuable information on the rate of gelation (but not on the actual final gel strength) of alginate-containing foods in the human gastric lumen.

1. Introduction

Alginates are unbranched block co-polymers of (1 → 4)-linked residues of β-D-mannuronic (M) acid and α-L-guluronic (G) acids. Two main types of gel with contrasting properties can be obtained which are referred to as ionic and acid gels. In the absence of multivalent ions when the pH of the alginate solution falls below the pKa value of the uronic acid groups (pKa = −log(Ka) where Ka is the acid ionization constant; pKa mannuronic acid = 3.38; pKa guluronic acid = 3.65) they become protonated. This reduces the electrostatic repulsion between the alginate polymer chains allowing hydrogen bonds to be created, which results in a weak acid alginate gel being formed (Draget, Skjåk-Bræk, Christensen, Gaserod, & Smidsrød, 1996; Draget, Skjåk-Bræk, & Stokke, 2006; Draget, Stokke, Yuguchi, Urakawa, & Kajiwara, 2003). Conversely, in the presence of multivalent ions such as Ca^{2+}, ionic bonds are created according to the egg-box model (Braccini & Perez, 2001) and much stronger ionic alginate gels are formed (Draget, Simensen, Onsoyen, & Smidsrød, 1993; Stokke et al., 2000).

There has been increasing interest in studying the properties of alginate gels *in vitro* and *in vivo* due to the wide range of their applications (Draget et al., 1993). The research interest has been focused mainly on ionic alginate gels due to their wide range of application, for example as biomaterials to encapsulate bio-molecules (Draget et al., 1993; Shen et al., 2003; Vogelsang, Wijffels, & Ostgaard, 2000), to support implanted organs (Smidsrød & Skjåk-Bræk, 1990), and to provide gastric anti-acid reflux drugs (Mandel, Daggy, Brodie, & Jacoby, 2000). Alginates are also widely used as thickeners by the food industry (Rinaudo, 2002). In this field acid alginate gels may play an additional role due to their property of gelling under acid conditions such as those found in the human stomach. This is potentially important since increased meal viscosity in the stomach can delay gastric emptying, increase the sense of satiety, and also delay absorption of nutrients (Bergmann et al., 1992; Cherbut, Albina, Champ, Doublier, & Lecannu, 1990; Dilorenzo, Williams, Hajnal, & Valenzuela, 1988; Marciani et al., 2000; Prove & Ehrlein, 1982).

Nuclear magnetic resonance (NMR) relaxometry has been used previously to study non-invasively the gel microstructure and gelation dynamics of alginates. In particular, the NMR transverse relaxation time $T2$ of the water protons in gels is a sensitive indicator of the state of gelation (Ablett, Lillford, Baghdadi, & Derbyshire, 1978; Degrassi, Toffanin, Paoletti, & Hall, 1998; Duez et al., 2000; Hills et al., 2000). The measured value of $T2$ is a combination of several factors, e.g. the mobility of the water protons (^{1}H), the concentration of macromolecules in the sample, the exchange of protons between the water and the macromolecules, as well as the local magnetic environment of the sample. There is extensive liter-

* Corresponding author. Tel.: +44 115 951 4747; fax: +44 115 951 5166.
E-mail address: Penny.Gowland@nottingham.ac.uk (P.A. Gowland).
[1] Now at University FAU Erlangen-Nürnberg, Germany.
[2] Now at University of Birmingham, UK.

0144-8617/$ – see front matter © 2010 Elsevier Ltd. All rights reserved.
doi:10.1016/j.carbpol.2010.05.033

ature investigating the NMR proton relaxation properties of ionic alginate gels (Degrassi et al., 1998; Duez et al., 2000; Hills et al., 2000), for example how *T*2 changes with alginate concentration (Potter, Carpenter, & Hall, 1993) and calcium ion content (Potter, Balcom, Carpenter, & Hall, 1994).

Previous rheological studies have shown that the gel strength of ionic gels can be correlated with calcium concentration and the percentage of guluronic acid groups present in the alginate chain (Braccini & Perez, 2001; Draget et al., 2003). Previous NMR relaxometry studies *in vivo* have also shown that valuable information can be gained on the gastrointestinal fate and performance in the gastric lumen of weak alginate-based meals (Hoad et al., 2004). Recent work also characterised the *T*2 of alginate beads as an encapsulation matrix *in vitro* and *in vivo* (Hoad et al., 2009; Rayment et al., 2009). However, to our knowledge, little data is available relating NMR relaxometry to the rheology of acid alginate gels. Although acid gels are utilised in some food and pharmaceutical applications, they are commercially less important than ionic gels, probably due to the weak gels they form. However, in acidic conditions when the carboxyl groups become protonated such as in the gastric environment, these gels become scientifically more relevant.

This study aimed to investigate *in vitro* the relationship between NMR relaxometry and the rheology of acid and ionic alginate gels prepared from a commercial food grade alginate. For some of the NMR relaxometry studies we also used a whole-body human magnetic resonance imaging (MRI) scanner (which measures *T*2 at relatively long echo times, but with relatively homogeneous B_1 and B_0 fields) in order to be able to better relate the *in vitro* findings to future *in vivo* studies aimed to assess the fate of alginate-containing foods in the gastric lumen during digestion.

2. Materials and methods

2.1. Alginate solutions

Food grade sodium alginate (Manugel DMB) was obtained from ISP Alginates (Tadworth, UK). The average molecular weight of the alginate was determined to be 2.83×10^5 Da using HPSEC-MALLS and the guluronic acid residue content was found to be 72% using ^{1}H NMR analysis (Grasdalen, 1983). Alginate solutions were prepared by dissolving 0.5–2.0% (w/w) of alginate powder in de-ionised water as follows: 500 ml of water was initially heated up to 80 °C in a beaker using a heater/stirrer. Whilst maintaining this temperature, the alginate powder was added slowly whilst the water was stirred vigorously for approximately 15 min. The solution was then removed from the heat and stirred for 1 h to allow complete dissolution of the alginate. The alginate solution was then left to cool until it reached room temperature.

2.2. Acid alginate gels

Formation of the 0.5–2% (w/w) acid alginate gels was obtained by vigorously stirring the corresponding alginate solution and adding 14% (w/w) of glucono-δ-lactone powder (GDL, Sigma–Aldrich, UK) to the solutions. When GDL is dissolved in water, it dissociates and releases protons in solution. When the concentration of protons is large enough to decrease the pH of the solution below the pKa value of uronic groups on the alginate chains (pKa guluronic acid = 3.65, pKa mannuronic groups = 3.38), they become protonated and hydrogen bonds form between the polymer chains producing weak acid gels.

Stirring was stopped as soon as all the GDL was dissolved (~30 s) and the pH was monitored continuously with a pH Turtle meter (Hanna Instruments Ltd, Bedfordshire, UK) until it reached a pH of ~2.5 (usually within 15 min). The acid alginate gels produced were opaque in appearance. They were then placed in 150 ml jars, laboratory sample tubes or cylindrical Teflon moulds, depending on the type of experiment to be subsequently performed on them, and stored in an oven at 37 °C for over 24 h. A temperature of 37 °C was chosen to mimic the temperature in the human digestive tract, and the 24 h wait allowed the dynamic gelation process to have reached an equilibrium state.

2.3. Ionic alginate gels

0.5–3% (w/w) alginate solutions were initially prepared as described above. The insoluble calcium salt tri-calcium phosphate (TCP, type C13-13, CF Budenheim, Germany) was then dispersed into these solutions at concentrations between 0.075% and 0.465% (w/w). This was followed by addition of GDL whilst stirring vigorously for just a few seconds to allow it dispersion, which resulted in a reduction in the pH of the solution allowing calcium ions to be solubilised from the TCP (Ström & Williams, 2003). Sufficient GDL to dissociate 75% of the Ca^{2+} ions was added (measured with a Ca meter Model 93-20, Orion Research, Incorporated Lab Products). As long as the concentration of H^+ does not decrease below the pKa value of the alginate, then the divalent calcium ions bind to the G residues of the alginate polymer via ionic bonds forming a three-dimensional network. The kinetics of formation of these gels is controlled by the rate of acidification and hence by the amount of GDL added to the solution.

The Ca^{2+} concentration is presented in terms of the parameter *R* according to the "egg-box model" (Grant, Morris, Rees, Smith, & Thom, 1973). *R* indicates the fractional saturation of binding sites on the alginate once the gel is created (Ström & Williams, 2003). It is given by the expression (Durand et al., 1988):

$$R = \frac{2[Ca^{2+}]}{[COO^-]}, \quad (1)$$

where $[Ca^{2+}]$ is the calcium ion concentration and $[COO^-]$ is the concentration of uronic acid residues on an alginate chain. The ionic alginate gels obtained were transparent in appearance. They were stored according to the procedure described for the acid gels. The pH was monitored measured during this process to ensure that the resulting gels had a pH value above the pKa values (3.65) for the uronic acid groups on the alginate.

2.4. Rheology measurements

The storage modulus (G') was measured using a Paar Physica UDS200 rheometer (Anton Paar, UK). A time sweep was conducted at a stress of 0.1 Pa and an oscillating frequency of 1 s^{-1} over a period of 24 h. The experiments were performed at 37 °C with a MP31 (50 mm diameter) parallel plate configuration and a gap of 1 mm. Slip between sample and rheometer plates was minimised by sticking emery paper with superglue to the upper and lower plates. A thin layer of silicon oil was applied to the exposed surface of the sample to minimise desiccation.

Compression tests were performed using an Instron Universal Testing Machine (Instron, High Wycombe, UK). The samples were prepared in cylindrical Teflon moulds of dimensions 12 mm × 12 mm and stored at 37 °C for 24 h. The moulds had been greased with olive oil to assist extraction of the samples. Experiments were performed using either a 10 or 100 N load cell, depending on the nature of the sample, with a crosshead speed of 10 mm/min. Experiments were performed on 10 different samples for each gel and concentration. Force-displacement data were converted into true stress/strain plots using the sample dimensions, where stress = force/area and strain = displacement/original length.

Gel "hardness" or stress to break the gels was determined from the maximum peak on the stress–strain plots.

2.5. NMR relaxometry measurements

The water proton relaxation time $T2$ was measured as a function of time to characterise the dynamics of gelation over a time period of 24 h. These measurements were performed on a 0.5 T MARAN instrument operating at a proton resonance frequency of 23 MHz (Resonance Instruments Ltd, Oxford, UK) using the Carr-Purcell-Meiboom-Gill (CPMG) pulse sequence employing a 2.8 μs 90° pulse length and a 5.5 μs 180° pulse length, with a pulse spacing of 500 μs, repetition time (TR) of 5 s and 4 averages per data point. Approximately 1 ml of solution was placed in a 10 mm o.d. glass tube. Measurements were recorded every 60 s. $T2$ values were calculated by fitting the decay of the echo amplitudes to a mono-exponential model using a weighted linear fitting algorithm (Resonance Instruments, WINFIT software). The samples were kept at 37 °C throughout the experiment using the manufacturer's temperature control unit.

Water proton NMR relaxation times measurements were also performed using a home-built 0.5 T whole-body scanner (gradient rise times under 400 μs, body transmit/receive coil 90 cm diameter) after the samples had been stored for 24 h at a temperature of 37 °C. $T2$ measurements were performed using a single spin-echo echo-planar imaging (EPI) sequence repeated 8 times with echo time values between 64 and 1564 ms and TR = 15 s. The image matrix was 128 × 128, the imaging slices were 1 cm thick and the in-plane resolution 4 mm × 3 mm. $T2$ values were calculated by a weighted linear fit using a custom-written program in IDL (Research Systems Inc., Boulder, Colorado, USA). The longitudinal relaxation time $T1$ measurements were performed using an Inversion Recovery-EPI sequence, with 8 inversion times (TI) varying from 1 to 15 s quadratically spaced and TR = 15 s. The image matrix was 128 × 128, the slices were 1 cm thick and the in-plane resolution was 4 mm × 3 mm. $T1$ values were calculated by fitting the measured signal at each inversion time ($S(TI)$) to the following expression:

$$S(TI) = S_0(1 - 2e^{-TI/T1}), \quad (2)$$

where S_0 is the equilibrium signal from the sample. S_0 and $T1$ were estimated by minimising the sum of squares difference of expected and measured signal values using the solver application from Excel (Microsoft Office applications).

The samples were placed in cylindrical beakers with a diameter of 12 cm and a height of 20 cm, covered with a plastic film. For each $T1$ and $T2$ measurement session five beakers were placed inside the whole-body scanner and they were kept at 37 °C using a custom-built water bath. Each experiment was repeated five times using five different batches of gel at the respective concentrations. The data for $T1$ and $T2$ analysis was obtained for regions of interest placed in the middle of the beaker and comprising approximately 25 voxels.

3. Results

3.1. pH Measurements

The time dependent change in pH during the formation of an acid and an ionic 1% (w/w) alginate gel is shown in Fig. 1. The decrease in pH was much greater for the acid gels (pH ~2 after 50 min) compared to the ionic gels (pH ~5.4 after 50 min). In both cases the major changes in pH occurred in the first 500 s. After this time the pH values for the ionic and acid gels begin to reach a steady plateau.

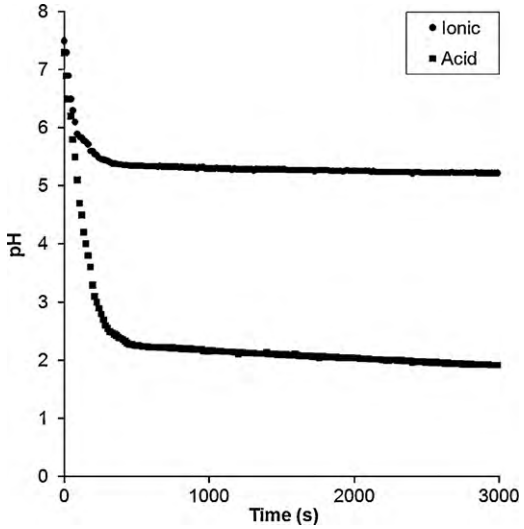

Fig. 1. Time dependent changes in pH during the formation of 1% (w/w) acid and ionic alginate gels. The acid gel was formed by adding 14% (w/w) of GDL to the alginate solution. The ionic gel was formed by adding 0.236% (w/w) of GDL to the alginate solution which also contained 1.5 g/l of TCP.

3.2. Rheology measurements

The time dependent changes in the storage modulus (G') during the formation of the ionic and acid gels at the two alginate concentrations of 0.75% and 1.5% (w/w) are shown in Fig. 2. There were initial plateaus in the time dependence of the G' for both the 1.5% acid and 1.5% ionic samples, whereas the G' values for the corresponding lower concentration samples were initially too low for meaningful measurements to be recorded. After a period of ~2 min the G' value for the 0.75% and 1.5% acid gel samples both started to increase rapidly with time. In contrast the ionic samples did not show a rapid increase in G' until after ~20 min. These time dependent increases in G' then continued for all four samples until they all reached a final limiting value of ~500 Pa.

The compression test data (stress as a function of applied strain) are shown in Fig. 3. The mean gel hardness values are displayed in Table 1.

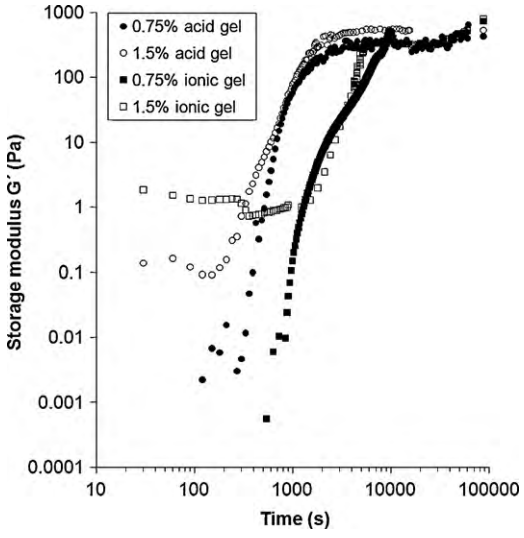

Fig. 2. Time dependence of the storage modulus (G') during the formation of 0.75% and 1.5% (w/w) acid and ionic alginate gels at 37 °C.

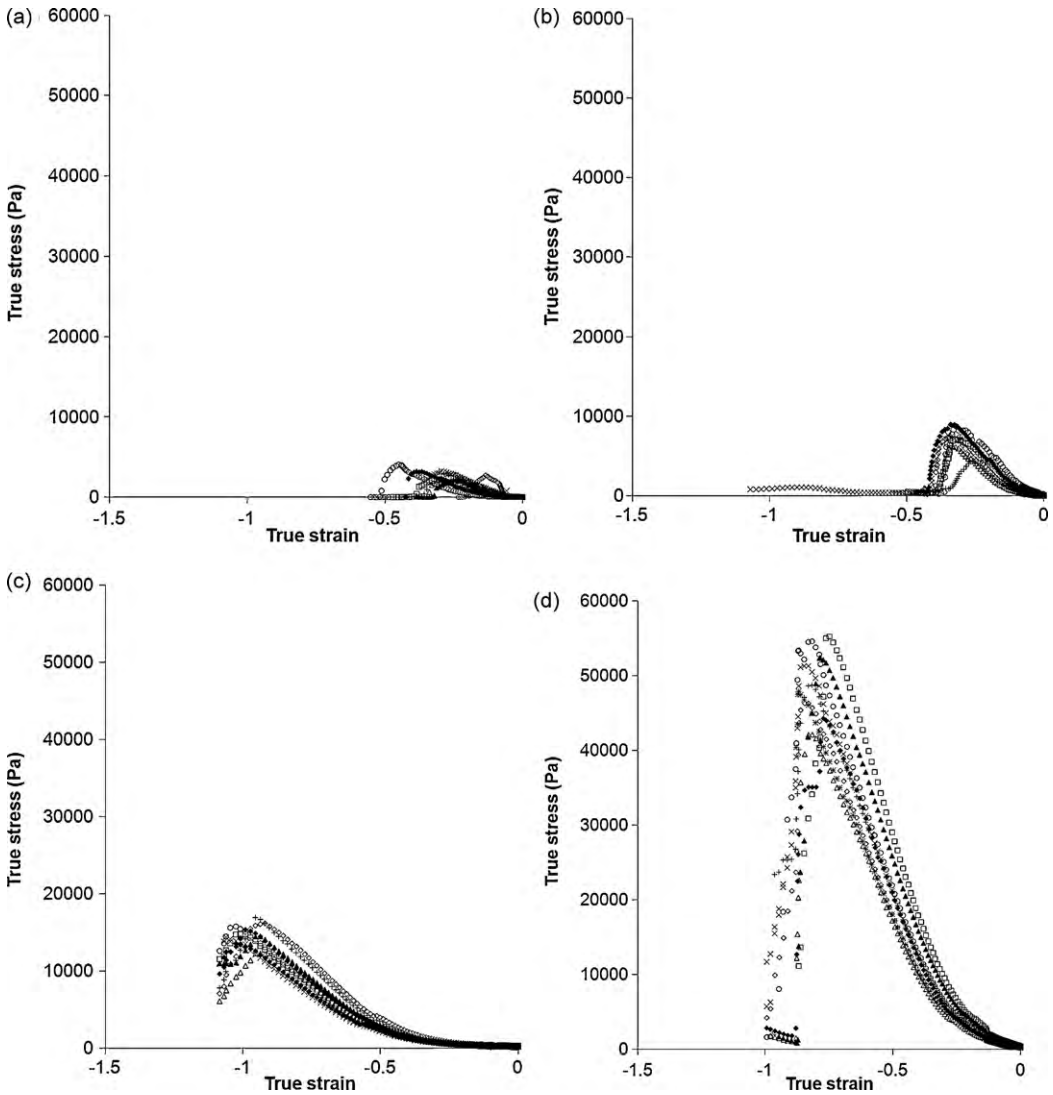

Fig. 3. True stress calculated from the compressive force applied to 12 mm diameter cylinders of (a) 0.75% (w/w) acid, (b) 1.5% (w/w) acid, (c) 0.75% (w/w) ionic and (d) 1.5% (w/w) ionic gels as a function of applied true strain.

3.3. NMR relaxometry measurements

The time dependent changes in the NMR transverse relaxation rate $R2$ ($R2 = 1/T2$) for 0.75% and 1.5% (w/w) ionic and acid gels measured using the MARAN bench-top spectrometer are shown in Fig. 4. For all four samples there was initially no significant change in the $R2$ value. After ~10 min there was an increase of the $R2$ value for both acid samples. In contrast to this the $R2$ values for the ionic samples did not start to increase until after ~30 min. This increase was less steep for the ionic samples compared to the acid samples and lasted for a much longer period of time (i.e. ~4 and ~8 h for

Table 1
Maximum stress values calculated from the applied breaking force for 1.5% and 0.75% (w/w) ionic and acid alginate gels, and the corresponding NMR $R2$ values (taken from the linear regression fits to the data shown in Fig. 5). All measurements were carried out at 37 °C on gels stored for 24 h.

Gel	Gel hardness (Pa)	NMR $R2$ (s^{-1})
1.5% Ionic	$(4.9 \pm 0.4) \times 10^4$	3.8 ± 0.4
1.5% Acid	$(0.8 \pm 0.1) \times 10^4$	3.4 ± 0.3
0.75% Ionic	$(1.5 \pm 0.13) \times 10^4$	1.9 ± 0.6
00.75% Acid	$(0.3 \pm 0.06) \times 10^4$	2.3 ± 0.2

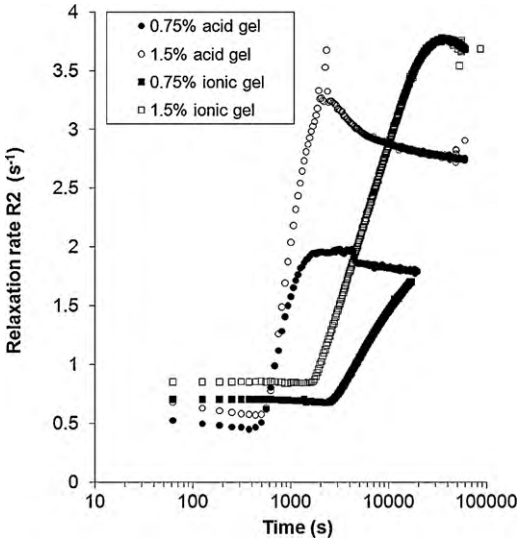

Fig. 4. Time dependent changes in the $R2$ NMR relaxation rate of the water during the formation of 0.75% (w/w) and 1.5% (w/w) acid and ionic gels. Measurements were recorded at 37 °C using the 0.5 T MARAN NMR spectrometer.

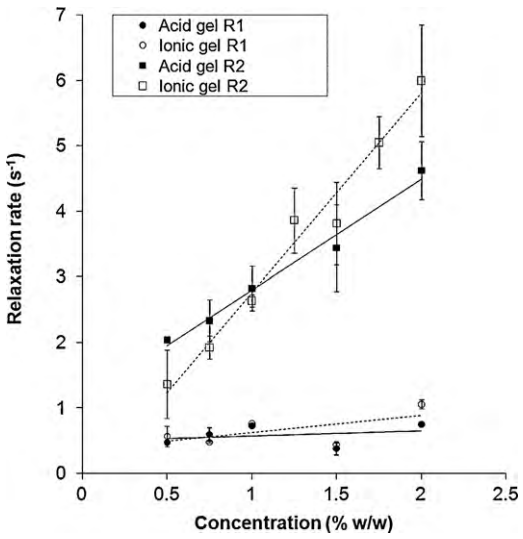

Fig. 5. *R*1 and *R*2 NMR relaxation rates of the water as a function of alginate concentration for acid and ionic gels at 37 °C. Measurements were recorded after 24-h sample storage using the whole-body 0.5 T MRI scanner. Lines represent the associated best linear fits to the data.

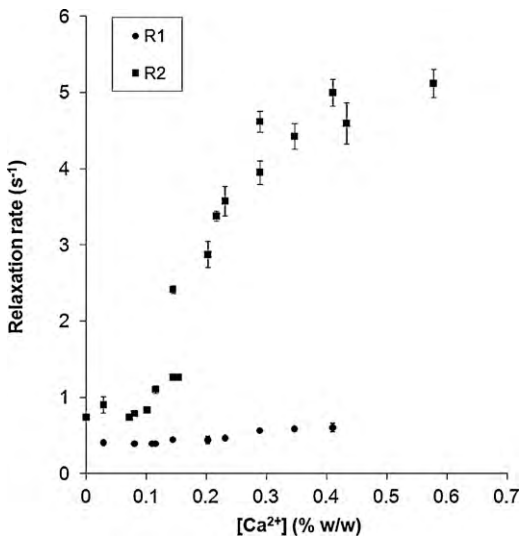

Fig. 6. *R*1 and *R*2 NMR relaxation rates of the water in a 1.5% (w/w) alginate gel as a function of Ca^{2+} concentration (w/w) at 37 °C. Measurements were recorded after 24-h storage using the whole-body 0.5 T MRI scanner.

the 0.75% and 1.5% ionic samples respectively, compared with only 15 and 30 min for the 0.75% and 1.5% acid samples). The 0.75% and 1.5% acid gels reached maximum *R*2 values of ~1.9 and ~3.2 s^{-1}, respectively, after which they both reduced slightly with time. The 1.5% ionic gel showed a similar trend and reached a maximum *R*2 value of ~3.2 s^{-1}, whereas the 0.75% ionic gel did not reach a maximum during the observation time, which is probably due to the long gelling time of this sample.

The NMR relaxometry measurements of the gels carried out at 24 h using the whole-body scanner are shown in Fig. 5. This shows the measured NMR transverse relaxation rate *R*2 and the longitudinal relaxation rate *R*1 (*R*1 = 1/*T*1) of water protons as a function of alginate concentration. *R*1 showed only a very limited increase as a function of alginate concentration from 0.5% to 2.0% (w/w), with the *R*1 values starting at 0.47 s^{-1} and reaching a maximum of 1.0 s^{-1}. In contrast to this, *R*2 showed a more marked increase with alginate concentration. The *R*2 values for ionic gels started at 1.3 s^{-1} at 0.5% alginate, and increased up to a value of 5.9 s^{-1} at 2.0% alginate. The corresponding change in *R*2 values for an acid gel increased from 2.0 to 4.6 s^{-1}. The values of the gradients of the *R*2 curves were 3.0 (*R*2 = 0.9756) and 1.7 s^{-1}/polymer concentration (w/w) (*R*2 = 0.9836) for ionic and acid samples, respectively.

Finally, Fig. 6 shows the changes in *R*1 and *R*2 values as a function of (w/w) Ca^{2+} concentration for 1.5% ionic gels at the 24 h time point. *R*2 can be seen to be much more sensitive to changes in Ca^{2+} concentration compared to the corresponding *R*1 values. The initial *R*2 value was 0.8 s^{-1} and this did not change significantly with increasing calcium content up to a Ca^{2+} concentration of ~0.15% (w/w), corresponding to *R* ~ 0.3. *R*2 then increased with calcium concentration until it reached a final *R*2 value of 5.0 s^{-1} at a concentration of ~0.5% (w/w) (*R* ~ 1). In contrast to this, the measured *R*1 value of 0.5 s^{-1} did not change significantly over the same corresponding concentration range.

4. Discussion

4.1. Formation of acid and ionic gels

Two types of alginate gels can be formed, i.e. acid and ionic gels, depending on the experimental conditions. Acid gels are created by reducing the pH below the pKa of the uronic groups to allow hydrogen bonds to form between adjacent alginate chains, whereas ionic gels are formed by adding multivalent ions (typically calcium) to form ionic bonds between adjacent alginate chains. In both cases simply adding the acid or calcium to an alginate solution would not produce a uniform gel structure. Preparing these types of gels requires the gelling agent to be added in a controlled manner and uniformly throughout the alginate solution. In the case of the acid gels this can be done by dispersing GDL powder in the alginate solution. As the GDL dissolves, it dissociates and releases protons uniformly throughout the alginate solution. When sufficient GDL is added to lower the pH below the pKa value of the uronic groups on the alginate chains acid gels are produced. GDL can also be used in the production of the ionic gels. In this case TCP is initially dispersed in the alginate solution prior to GDL. Less GDL is added to form the ionic gels compared to the amount used for the acid gels because the pH only needs to decrease sufficiently to allow the calcium ions to dissociate from the TCP and form divalent ionic bonds between alginate chains. The time dependent changes in pH observed during the formation of the 1% (w/w) acid and ionic alginate gels are shown in Fig. 1. This figure highlights how the pH of the alginate solution remained above the pKa value (pH >3.5) for the formation of the ionic gels, and below it (pH <3.5) for the formation of the acid gels. Significant changes in the pH are observed in the initial 500 s; thereafter the pH values begin to reach a steady plateau.

4.2. Rheology measurements

The time dependence of the storage modulus (Fig. 2) for all the samples showed G' to increase by 3–4 orders of magnitude during the formation of the gel structures. The gels prepared using a higher concentration of alginate (1.5%, w/w) displayed an initial plateau in G' which may be due to a fast initial structuring of these systems caused by the higher concentration of binding sites. However the acid gels appeared to reach a maximum plateau in G' quicker than the corresponding ionic gels (~45 min versus ~120 min, respectively). This is as expected since acid gels should form more quickly because a higher level of GDL is used for their production. In addition, ionic gels require the subsequent release of calcium ions from the TCP before the ionic bonds can start to form. The results in Fig. 2 also indicate that all the gels had a similar final G' values of ~500 Pa. The stronger ionic gels would be expected to have significantly higher G' values compared to the correspondingly weaker

acid gels. Draget, Skjåk-Bræk, and Smidsrød (1994) report G' values of above 200 Pa for a 1% alginic acid gel prepared from a *Laminaria hyperborea* leaf alginate with similar guluronic acid residue content (70%). It is well known that the strength of ionic alginate gels increase with increasing divalent cation concentration (Ouwerx, Velings, Mestdagh, & Axelos, 1998). This final limiting G' value may have been affected by the gel drying out despite a thin layer of silicon oil being applied to the exposed surface of the sample to minimise desiccation. Therefore these small deformation experiments were used primarily to study the onset and early stages of the gelation process.

The material properties of the final gels produced were investigated by large deformation experiments using the Instron universal testing machine. The maximum stress values for the 1.5% and 0.75% (w/w) ionic gels measured using this technique can be seen in Table 1 to be significantly larger than the corresponding values for the acid gels. These results showed that the gel strength of the ionic gels was significantly greater than for corresponding acid gels as expected (Draget et al., 1993; Stokke et al., 2000).

4.3. NMR relaxation measurements

The time dependent changes in the NMR $R2$ values (Fig. 4) showed similar trends to those observed in the G' storage modulus (Fig. 2): there was an initial plateau region which was shorter for the acid gels compared to the ionic gels (10 min compared to 30 min, respectively). However, the length of the plateau region was slightly longer for the NMR compared to the G' data. This is thought to be due to the slightly longer time it took to load the samples in the rheometer for the G' measurements. After this initial time period, $R2$ significantly increased with time for acid and ionic gels. The rate of change in $R2$ was greater for both acid gels compared to the corresponding ionic gels. Similar trends were observed in the rate of change in G' (Fig. 2), and again this is interpreted as showing that the acid gels form more quickly than the corresponding ionic gels since the ionic gel formation is reliant on the time dependant release of Ca^{2+} from the TCP using GDL. The final $R2$ values measured for both the 0.75% acid and ionic gels were similar (although ionic gel was still changing). At the higher alginate concentration of 1.5% the final $R2$ value of the ionic gel was greater than the corresponding value for the acid gel, although both values were greater than the corresponding $R2$ values at the lower concentration of 0.75%. These results showed that the $R2$ relaxation was sensitive to both the concentration of the alginate present, as well as the type of gel formed. However, whilst the NMR $R2$ parameter was sensitive to the gelation process, it was not directly related to the actual strength of the gel. This is not a surprising since the gel strength is a bulk macroscopic material property, whereas the NMR $R2$ relaxation rate probes molecular dynamics on a much smaller microscopic scale. Specifically $R2$ is reporting on changes in molecular mobility of the alginate chains as the cross-links are forming during the gelation process, whilst G' is reporting on how these cross-links are changing the bulk material properties of the sample. The $R2$ values depend on rapid exchange, on the NMR timescale, between labile hydroxyl protons of the alginate and the water protons, with the measured value being a population weighted average of their respective $R2$ values (Zimmerman & Brittin, 1957), and this relationship is shown in Eq. (3):

$$Ri_{meas} = P_a Ri_a + P_b Ri_b, \tag{3}$$

where Ri_{meas} is the measured Ri value, Ri_a is the Ri of the water protons, Ri_b is the Ri for the labile protons of the alginate, P_a is the relative population of water protons, P_b is the relative population of alginate labile protons with $P_a + P_b = 1$ and $i = 1$ or 2 referring to either $R1$ or $R2$ relaxation rates. Eq. (3) highlights why the measured $R2$ was sensitive to both alginate concentration (i.e. changes in P_b) and the gelation process (i.e. changes in $R2_b$). The non-exchangeable alginate protons are not considered to contribute because their signal decays very rapidly and it would have most likely decayed completely before the CPMG signal had been initially sampled and even if it had not completely decayed, its contribution would still be very small compared to the overall total signal intensity.

Diffusion of water molecules in inhomogeneous magnetic fields (either arising from imperfect shimming or susceptibility variations in the sample) will lead to unrecoverable spin dephasing. The CPMG sequence was designed to remove these diffusion effects from standard $T2$ measurements, and is considered to be the gold standard measurement technique for $T2$. However the CPMG sequence is very sensitive to variations in the amplitude of the RF pulse, and such RF variations are difficult to eliminate *in vivo*. Therefore *in vivo* where the effect of RF pulse errors are more problematic than the effect of diffusion in poorly shimmed fields, the most robust measurements of $T2$ are made with the Hahn echo sequence. Because of this, slight differences in the measured $R2$ values between the bench-top NMR and the whole-body scanner are to be expected as seen for example in the $R2$ values of the acid gels in Figs. 4 and 5.

The NMR $R1$ relaxation rates measured using the body scanner for both the ionic and acid gels (Fig. 5) are less sensitive to changes in polymer concentration than the corresponding $R2$ relaxation rate. This difference in the concentration dependence of $R1$ and $R2$ is in agreement with previous work on ionic gels (Degrassi et al., 1998).

The change in $R1$ and $R2$ values as a function of calcium ion concentration for the ionic gels is shown in Fig. 6. $R2$ was again the most sensitive NMR parameter, and Eq. (3) can be used to explain the observed changes in $R2$ with increasing calcium concentration. The only variable that is expected to change with increasing calcium concentration is $R2_b$ due to the decreased molecular mobility of the alginate chains as a result of the increased number of cross-links formed. Therefore the observed changes in the measured $R2$ value shown in Fig. 6 were considered to be directly related to changes in mobility of the alginate chains. Initially only a minimal increase in $R2$ up to a calcium ion concentration R value of 0.25 was observed (where R is the fractional saturation of binding sites on the alginate once the gel is created (Eq. (1))). At this low calcium concentration it is unlikely that there would be sufficient ionic cross-links to form a gel network, so $R2_b$ would be expected to only increase slightly in this calcium concentration region. The $R2$ value then increased significantly with increasing calcium up to an R concentration value of $R = 1$, after which $R2$ again became much less sensitive to increasing calcium concentration. There are likely to be sufficient ionic cross-links for a gel network to start to form above a calcium R concentration of 0.25, which means $R2_b$ would start to increase significantly with increasing calcium concentration. Once the calcium concentration reached $R = 1$ then all the potential binding sites on the alginate would be occupied, and $R2_b$ would be expected to become invariant again with further increases in calcium content. However, $R2$ can be seen to continue to increase slightly with increased calcium concentration above $R = 1$ (Fig. 6). This could possibly be due to the onset of syneresis. Syneresis is the expulsion of water due to contraction of the gel network, and so it would result in a slight time dependent increase in gel concentration. This change in gel concentration would result in a corresponding time dependent change in the relative populations P_a and P_b in Eq. (3).

5. Conclusions

We have shown how measurements of the time dependent change in the storage modulus (G') can be used to characterise the gelation process of these two types of alginate gels. Compression tests on the final gels created have confirmed that acid gels

are much weaker than the corresponding ionic gels. Similar time dependent changes in the NMR *R*2 relaxation rate of the water during the formation of the gels are also reported, which demonstrates how this NMR parameter can be used as a non-invasive/non-destructive means of measuring the formation of these types of alginate gels. This is an important finding because it shows that the NMR *R*2 relaxation rate could be used in *in vivo* MRI studies to follow the fate of alginate-containing foods in the human gastric lumen (Hoad et al., 2004; Hoad et al., 2009). However, it should be noted that there was no correlation between the measured NMR *R*2 value and the final gel strength for the different types of alginate gels studied (Table 1). Therefore, although *in vivo R*2 measurements could provide valuable information concerning the rate of gelation in the human gastric lumen, they would not be able to provide corresponding information on the actual strength of the final gel produced.

References

Ablett, S., Lillford, P. J., Baghdadi, S. M. A., & Derbyshire, W. (1978). Nuclear magnetic resonance investigation of polysaccharide films, sols and gels. 1. Agarose. *Journal of Colloid and Interface Science*, *67*(2), 355–377.

Bergmann, J. F., Chassany, O., Petit, A., Triki, R., Caulin, C., & Segrestaa, J. M. (1992). Correlation between echographic gastric-emptying and appetite – influence of psyllium. *Gut*, *33*(8), 1042–1043.

Braccini, I., & Perez, S. (2001). Molecular basis of Ca^{2+}-induced gelation in alginates and pectins: The egg-box model revisited. *Biomacromolecules*, *2*(4), 1089–1096.

Cherbut, C., Albina, E., Champ, M., Doublier, J. L., & Lecannu, G. (1990). Action of guar gums on the viscosity of digestive contents and on the gastrointestinal motor function in pigs. *Digestion*, *46*(4), 205–213.

Degrassi, A., Toffanin, R., Paoletti, S., & Hall, L. D. (1998). A better understanding of the properties of alginate solutions and gels by quantitative magnetic resonance imaging (MRI). *Carbohydrate Research*, *306*(1–2), 19–26.

Dilorenzo, C., Williams, C. M., Hajnal, F., & Valenzuela, J. E. (1988). Pectin delays gastric-emptying and increases satiety in obese subjects. *Gastroenterology*, *95*(5), 1211–1215.

Draget, K. I., Simensen, M. K., Onsoyen, E., & Smidsrød, O. (1993). Gel strength of Ca-limited alginate gels made in-situ. *Hydrobiologia*, *261*, 563–569.

Draget, K. I., Skjåk-Bræk, G., Christensen, B. E., Gaserod, O., & Smidsrød, O. (1996). Swelling and partial solubilization of alginic acid gel beads in acidic buffer. *Carbohydrate Polymers*, *29*(3), 209–215.

Draget, K. I., Skjåk-Bræk, G., & Smidsrød, O. (1994). Alginic acid gels: The effect of alginate chemical composition and molecular weight. *Carbohydrate Polymers*, *25*, 31–38.

Draget, K. I., Skjåk-Bræk, G., & Stokke, B. T. (2006). Similarities and differences between alginic acid gels and ionically crosslinked alginate gels. *Food Hydrocolloids*, *20*(2–3), 170–175.

Draget, K. I., Stokke, B. T., Yuguchi, Y., Urakawa, H., & Kajiwara, K. (2003). Small-angle X-ray scattering and rheological characterization of alginate gels. 3. Alginic acid gels. *Biomacromolecules*, *4*(6), 1661–1668.

Duez, J. M., Mestdagh, M., Demeure, R., Goudemant, J. F., Hills, B. P., & Godward, J. (2000). NMR studies of calcium-induced alginate gelation. Part I. MRI tests of gelation models. *Magnetic Resonance in Chemistry*, *38*(5), 324–330.

Durand, D., Bertrand, C., Busnel, J. P., Emery, J. R., Axelos, M. A. V., Thibault, J. F., et al. (1988). Physical gelation induced by ionic complexation: Pectin-calcium systems. In W. Burchard, & S. B. Ross-Murphy (Eds.), *Physical Networks and Gels* (pp. 283–300). London, UK: Elsevier Applied Science.

Grant, G. T., Morris, E. R., Rees, D. A., Smith, P. J. C., & Thom, D. (1973). Biological interactions between polysaccharides and divalent cations: The egg-box model. *FEBS Letters*, *32*, 195–198.

Grasdalen, H. (1983). High-field ^{1}H-NMR spectroscopy of alginate: Sequential structure and linkage conformations. *Carbohydrate Research*, *118*, 255–260.

Hills, B. P., Godward, J., Debatty, M., Barras, L., Saturio, C. P., & Ouwerx, C. (2000). NMR studies of calcium induced alginate gelation. Part II. The internal bead structure. *Magnetic Resonance in Chemistry*, *38*(9), 719–728.

Hoad, C., Rayment, P., Cox, E., Wright, P., Butler, M., Spiller, R., et al. (2009). Investigation of alginate beads for gastro-intestinal functionality. Part 2. In vivo characterisation. *Food Hydrocolloids*, *23*(3), 833–839.

Hoad, C. L., Rayment, P., Spiller, R. C., Marciani, L., Alonso, B. D., Traynor, C., et al. (2004). In vivo imaging of intragastric gelation and its effect on satiety in humans. *Journal of Nutrition*, *134*(9), 2293–2300.

Mandel, K. G., Daggy, B. P., Brodie, D. A., & Jacoby, H. I. (2000). Review article: Alginate-raft formulations in the treatment of heartburn and acid reflux. *Alimentary Pharmacology and Therapeutics*, *14*(6), 669–690.

Marciani, L., Gowland, P. A., Spiller, R. C., Manoj, P., Moore, R. J., Young, P., et al. (2000). Gastric response to increased meal viscosity assessed by echo-planar magnetic resonance imaging in humans. *Journal of Nutrition*, *130*(1), 122–127.

Ouwerx, C., Velings, N., Mestdagh, M. M., & Axelos, M. A. V. (1998). Physico-chemical properties and rheology of alginate gel beads formed with various divalent cations. *Polymer Gels and Networks*, *6*, 393–408.

Potter, K., Balcom, B. J., Carpenter, T. A., & Hall, L. D. (1994). The gelation of sodium alginate with calcium ions studied by magnetic resonance imaging (MRI). *Carbohydrate Research*, *257*(1), 117–126.

Potter, K., Carpenter, T. A., & Hall, L. D. (1993). Mapping of the spatial variation in alginate concentration in calcium alginate gels by magnetic resonance imaging (MRI). *Carbohydrate Research*, *246*, 43–49.

Prove, J., & Ehrlein, H. J. (1982). Motor function of gastric antrum and pylorus for evacuation of low and high-viscosity meals in dogs. *Gut*, *23*(2), 150–156.

Rayment, P., Wright, P., Hoad, C., Ciampi, E., Haydock, D., Gowland, P., et al. (2009). Investigation of alginate beads for gastro-intestinal functionality. Part 1. In vitro characterisation. *Food Hydrocolloids*, *23*(3), 816–822.

Rinaudo, M. (2002). Alginates and carrageenans. *Actualite Chimique*, *11–12*, 35–38.

Shen, F., Poncet-Legrand, C., Somers, S., Slade, A., Yip, C., Duft, A. M., et al. (2003). Properties of a novel magnetized alginate for magnetic resonance imaging. *Biotechnology and Bioengineering*, *83*(3), 282–292.

Smidsrød, O., & Skjåk-Bræk, G. (1990). Alginate as immobilization matrix for cells. *Trends in Biotechnology*, *8*(3), 71–78.

Stokke, B. T., Draget, K. I., Smidsrød, O., Yuguchi, Y., Urakawa, H., & Kajiwara, K. (2000). Small-angle X-ray scattering and rheological characterization of alginate gels. 1. Ca-alginate gels. *Macromolecules*, *33*(5), 1853–1863.

Ström, A., & Williams, M. A. K. (2003). Controlled calcium release in the absence and presence of an ion-binding polymer. *Journal of Physical Chemistry B*, *107*(40), 10995–10999.

Vogelsang, C., Wijffels, R. H., & Ostgaard, K. (2000). Rheological properties and mechanical stability of new gel-entrapment systems applied in bioreactors. *Biotechnology and Bioengineering*, *70*(3), 247–253.

Zimmerman, J. R., & Brittin, W. E. (1957). Nuclear magnetic resonance studies in multiple phase system. Lifetime of a water molecule in an adsorbing phase on silica gel. *Journal of Physical Chemistry*, *61*(10), 1328–1333.